

Electronic Decay Constant of Carotenoid Polyenes from Single-Molecule Measurements

Jin He,[†] Fan Chen,[†] Jun Li,[†] Otto F. Sankey,[†] Yuichi Terazono,[‡] Christian Herrero,[‡] Devens Gust,[‡] Thomas A. Moore,[‡] Ana L. Moore,[‡] and Stuart M. Lindsay^{*,†,‡,§}

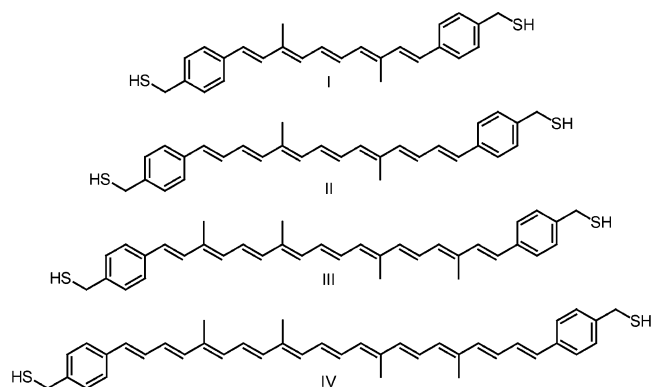
Department of Physics and Astronomy, Department of Chemistry and Biochemistry, and Biodesign Institute, Arizona State University, Tempe, Arizona 85287

Received November 8, 2004; E-mail: Stuart.Lindsay@asu.edu

Carotenoid polyenes have been used extensively as electron donors in molecular systems that demonstrate photoinduced electron transfer^{1,2} and have recently been found to act as electron shuttles in photosynthesis.^{3,4} Direct measurements of their conductance⁵ show that it is ca. 7 orders of magnitude higher than that of equivalent-length *n*-alkanes, as might be expected on theoretical grounds.⁶ This high conductivity should correspond to a small value of β , the electronic decay constant. A lower limit for β has been inferred from spectroscopic data obtained from intervalence charge-transfer complexes linked by polyenes,⁷ but β has not been measured directly. We have measured the conductance of a series of carotenoid polyenes as a function of their length, obtaining $\beta = 0.22 \pm 0.04 \text{ \AA}^{-1}$, in close agreement with the value obtained from first principles simulations ($0.22 \pm 0.01 \text{ \AA}^{-1}$).

The original measurements of the single-molecule conductance of a carotenoid polyene were made by inserting the molecule into an alkanethiol self-assembled monolayer and contacting the inserted molecules either directly with a conducting atomic force microscope (AFM) probe⁸ or by using a gold nanoparticle as an intermediate contact.^{5,9} Xu and Tao¹⁰ recently introduced a new method for single-molecule measurements based on repeated formation of break-junctions. Their method is much easier to use with various lengths of molecules and yields better data than the conducting AFM approach.¹¹

The homologous series of carotenoids (illustrated below) was synthesized as described in the Supporting Information.



The molecules consist of a polyene backbone of $N = 5$ (I), $N = 7$ (II), $N = 9$ (III), and $N = 11$ (IV) carbon-carbon double bonds in conjugation, each terminated with a benzene ring coupled to a thiol via a methylene linker. The role of the thiols is to bind to gold electrodes. A $2 \mu\text{M}$ solution of freshly deprotected molecules

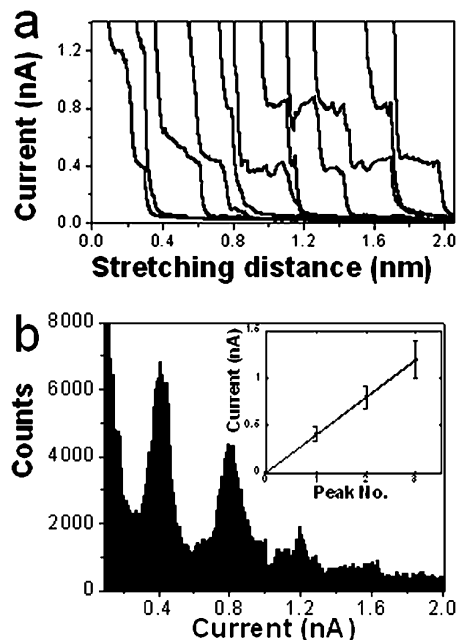


Figure 1. (a) Examples of current vs stretching distance data for I ($N = 5$) at a bias of 0.2 V. (b) Histogram of recorded currents shows peaks at ca. 0.4, 0.8, and 1.2 nA. The slope of a plot of peak value vs peak number (inset) yields the current per molecule.

in toluene was placed onto a hydrogen-flame-annealed Au(111) substrate¹² in the liquid cell of a scanning tunneling microscope (PicoSPM, Molecular Imaging, Tempe, AZ). After an hour, the substrate was rinsed thoroughly and submerged in toluene for measurement under Ar. Probes were made from freshly cut 0.25 mm Au wire (99.999%). The current was recorded on a digital oscilloscope as the probe was repeatedly pushed into and retracted from the substrate, with the tip-sample bias held fixed.¹⁰

Examples of current vs stretching distance (calculated from the known probe velocity) recordings in the presence of I are shown in Figure 1a. Taken at a fixed tip bias of 0.2 V, the traces show distinct steps at multiples of ca. 0.4 nA. These features are not observed without added molecules. A histogram of the recorded currents for hundreds of break-junctions (Figure 1b) shows a series of peaks corresponding to one, two, and three molecules in the gap.¹⁰ Fitting these histograms with Gaussians determines the peak centers and full widths at half-height (fwhh). These peak values are then plotted vs peak number (Figure 1b, inset), and the slope is determined using a least-squares fit, with the data points weighted using the fwhh as error bars. This slope determines the current at a fixed bias, and plots of current vs bias for all four molecules are shown in Figure 2. These current-voltage characteristics are linear over the measured range, and the slopes of these lines yield the

[†] Department of Physics and Astronomy.

[‡] Department of Chemistry and Biochemistry.

[§] Biodesign Institute.

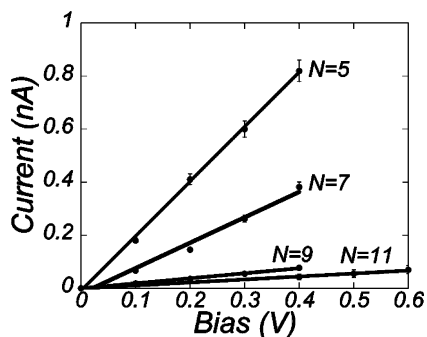


Figure 2. Current–voltage characteristics for the four carotenoids. Lines are linear fits, and error bars (not visible on most points) are ± 1 SE.

Table 1. Measured and Calculated Conductances (Hollow-Site Values Are in Parentheses)

N	G (measured) (nS)	G (calculated) (nS)
5	2.06 ± 0.05	7.84 (9.71)
7	0.96 ± 0.07	2.60 (3.55)
9	0.28 ± 0.02	0.89 (1.01)
11	0.11 ± 0.07	0.31 (0.30)

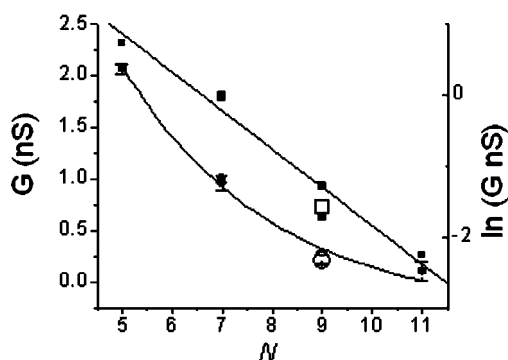


Figure 3. Conductance vs number of double bonds in conjugation on linear (circles) and log (squares) scales. Repeated data points are shown for $N = 7$ and $N = 9$ samples. Open symbols are data from ref 5.

molecular conductance data listed in Table 1 and plotted vs N in Figure 3. These data are well-fitted by an exponential decay, $G = G_0 \exp(-\beta_N N)$ (lines in Figure 3), with $\beta_N = 0.556 \pm 0.09$ and $G_0 = 37 \pm 18$ nS. The measured value for β_N , taken together with a linear distance between pairs of carbon atoms of 2.48 \AA (produced by the zigzag structure of a double bond of length 1.34 \AA and a single bond length of 1.45 \AA),¹³ leads to $\beta = 0.22 \pm 0.04 \text{ \AA}^{-1}$.

The structural geometry of each molecule was determined by energy minimization using Hartree–Fock theory¹⁴ for determination of bond lengths that are critical to the determination of electronic transmission.¹⁵ The molecule is linked via sulfur to ideal (111) Au surfaces at either the “hollow” site above a three Au atom junction or an “on-top” site directly above a single Au atom (as might be expected to occur for a molecule under tension as in the break-junction experiments¹⁰). The two approaches give some indication of the sensitivity of the result to local geometry. The currents were calculated as a function of applied bias as previously described.⁵

These current–voltage characteristics were linear in the range $0 < V < 0.6$ V, in good agreement with the experimental results, and the molecular conductances obtained from the slopes of these

characteristics are listed in Table 1. Values for bonding to an on-top site (the more appropriate geometry for the break-junction method) are well-fitted ($\chi^2 = 0.003$) by an exponential decay $G = G_0 \exp(-\beta_N N)$ with $\beta_N = 0.539 \pm 0.01$ and $G_0 = 115 \pm 6$ nS, yielding $\beta = 0.22 \pm 0.01 \text{ \AA}^{-1}$. Similar values are obtained using the calculated conductances for hollow-site bonding. The computed value of β is in better agreement with experiment than is the prefactor, G_0 . A partial explanation of this is that β is almost exclusively a property of the molecule and can be estimated even without having the molecule in contact with the metal.⁶ G_0 is sensitive to details of the molecule–metal interface, and this is probably not well-described by the flat surface used in our calculations.

Our previous measurement⁵ of the conductance of **III** ($N = 9$) yielded $G = 0.2$ nS, within 30% of the present measurement, justifying the interpretation of the break-junction histogram peaks in terms of single-molecule conduction.¹⁰ The somewhat lower value of current obtained with a nanoparticle contact⁹ is consistent with the trends observed in measurements of n -alkane conductance¹¹ caused by suppression of transmission owing to the electronic structure of the nanoparticle.

In summary, we have measured the electronic decay constant for carotenoid polyenes, finding a value in good agreement with the results of electronic structure calculations.

Acknowledgment. We thank Nongjian Tao for helping us to set up the break-junction apparatus. This work was supported by a NIRT grant (ECS 01101175) from the National Science Foundation.

Supporting Information Available: Sample preparation details. This material is available free of charge via the Internet at <http://pubs.acs.org>.

References

- Moore, T. A.; Gust, D.; Mathis, P.; Mialocq, J.-C.; Chachaty, C.; Bensasson, R. V.; Land, E. J.; Doizi, D.; Liddell, P. A. *Nature* **1984**, *307*, 630–632.
- Osuka, A.; Yamada, H.; Shinoda, T.; Nozaki, K.; Ohno, T. C. P. L. *Chem. Phys. Lett.* **1995**, *238*, 37–41.
- Vretos, J. S.; Steward, D. H.; de Paula, J. D.; Brudvig, G. W. *J. Phys. Chem. B* **1999**, *103*, 6403–6406.
- Faller, P.; Pascal, A.; Rutherford, A. W. *Biochemistry* **2001**, *40*, 6431–6440.
- Ramachandran, G. K.; Tomfohr, J. K.; Li, J.; Sankey, O. F.; Zarate, X.; Primak, A.; Terazano, Y.; Moore, T. A.; Moore, A. L.; Gust, D.; Nagahara, L. A.; Lindsay, S. M. *J. Phys. Chem. B* **2003**, *107*, 6162–6169.
- Tomfohr, J.; Sankey, O. F. *Phys. Rev. B* **2002**, *65*, 245105–245116.
- Woitellier, S.; Launay, J. P.; Spangler, C. W. *Inorg. Chem.* **1989**, *28*, 758–762.
- Leatherman, G.; Durantini, E. N.; Gust, D.; Moore, T. A.; Moore, A. L.; Stone, S.; Zhou, Z.; Rez, P.; Li, Y. Z.; Lindsay, S. M. *J. Phys. Chem. B* **1999**, *103*, 4006–4010.
- Cui, X. D.; Primak, A.; Zarate, X.; Tomfohr, J.; Sankey, O. F.; Moore, A. L.; Moore, T. A.; Gust, D.; Harris, G.; Lindsay, S. M. *Science* **2001**, *294*, 571–574.
- Xu, B.; Tao, N. J. *Science* **2003**, *301*, 1221–1223.
- Tomfohr, J.; Ramachandran, G.; Sankey, O. F.; Lindsay, S. M. Making Contacts to Single Molecules: Are We Nearly There Yet? In *Introducing Molecular Electronics*; Fagas, G., Richter, K., Eds.; Springer: Berlin, 2005.
- DeRose, J. A.; Thundat, T.; Nagahara, L. A.; Lindsay, S. M. *Surf. Sci.* **1991**, *256*, 102–108.
- Bart, J. C.; MacGillavry, C. H. *Acta Crystallogr.* **1968**, *B24*, 1587–1606.
- An STO basis set is used in the GAMESS program suite. Schmidt, M. W.; Baldridge, K. K.; Boatz, J. A.; Elbert, S. T.; Gordon, M. S.; Jensen, J. J.; Koseki, S.; Matsunaga, M.; Nguyen, K. A.; Su, S.; Windus, T. L.; Dupuis, M.; Montgomery, J. A. *J. Comput. Chem.* **1993**, *14*, 1347–1363.
- Tomfohr, J. K.; Sankey, O. F. *J. Chem. Phys.* **2004**, *120*, 1542–15554.

JA043279I